

***MFC-driven H<sub>2</sub>S electro-oxidation based on Fe nanoparticles anchored on carbon aerogel-ZIF-8: A collaborated experimental and DFT study***

Daryoush Sanaei<sup>1,2</sup>, Mohamadreza Massoudinejad<sup>1,2,\*</sup>, Muhammad Sufyan Javed<sup>3,7,\*</sup>, Saeed Motesaddi Zarandi<sup>1,2</sup>, Abbas Rezaee<sup>4</sup>, Hamidreza Sharifan<sup>5,6</sup>, Muhammad Imran<sup>7</sup>

<sup>1</sup>*School of Public Health and Safety, Shahid Beheshti University of Medical Sciences, Tehran, Iran*

<sup>2</sup>*Department of Environmental Health Engineering, Faculty of Public Health and Safety, Shahid Beheshti University of Medical Sciences, Tehran, Iran*

<sup>3</sup>*School of Physical Science and Technology, Lanzhou University, Lanzhou 730000, China*

<sup>4</sup>*Department of Environmental Health, Faculty of Medical Sciences, Tarbiat Modares University, Tehran, Iran*

<sup>5</sup> *Department of Chemistry and Forensic Science, Albany State University, Georgia, USA*

<sup>6</sup>*Air Quality Research Center, University of California, Davis, Davis, CA 95616-8521, USA*

<sup>7</sup>*Department of Chemistry, Faculty of Science, King Khalid University, P.O. Box 9004, Abha 61413, Saudi Arabia*

**Corresponding author**

[massoudi@sbmu.ac.ir](mailto:massoudi@sbmu.ac.ir)(M. Massoudinejad)

[muhammadsj@lzu.edu.cn](mailto:muhammadsj@lzu.edu.cn) (M.S. Javed)

## 1. Experimental Section

**Sample analysis:** The stability of catalyst on the electrode was evaluated with measuring of total dissolved metals in supporting electrolyte by plasma optical emission spectrometry (ICP-OES, Agilent 5100, Agilent Technologies). The Ion chromatography (IC, Dionex, USA) was used to measure dissolved HS<sup>-</sup>, S<sub>2</sub>O<sub>3</sub><sup>2-</sup>, and SO<sub>4</sub><sup>2-</sup>. For determination the formed concentration of polysulfide, against to the previous study that was used from H<sub>2</sub>O<sub>2</sub> at high pH as a method to measure the formed polysulfide (S1-S2), and in our study because the colloidal sulfur was a major product of oxidation reactions, then the gradual appearance of yellow color and the presence of soluble sulfur species in higher concentration due to further polysulfide oxidation were used as an indicator to calculate the formed polysulfide (S3). The electrochemical oxidation of elemental sulfur was presumed by measuring the total sulfide and the dissolved sulfur species. The first-order kinetics was used to fit data from measuring sulfide concentrations versus the initial sulfide concentrations

**Density functional theory (DFT) calculation:** The simulation package VASP and also the Projector Augmented Wave (PAW) method were carried out to calculate Density functional theory (DFT). For describing 3d Fe electrons, the PBE (U) method with the correlation energy (U) + exchange energy (J) under 4 eV and 1 eV, respectively, was conducted. The kinetic cutoff energy and the convergence criteria of energy were fixed to 450 eV and 10<sup>-4</sup> eV, and also the fixed force for geometry structures was chosen 0.01 eV Å<sup>-1</sup>. A Monkhorst-Pack mesh with a dimension of 3 × 3 × 1 with a space of nearly 10 Å was applied to the sample k-point of the Brillouin zone. The formation energy ( $E_{form}$ ) of Fe-doped CAs-ZIF-8@MM-MOF in different loading of Fe nanoparticles (1, 3, and 5% wt.) was determined as follows(S4-S6):

$$E_{form} = E(\text{Fe-doped-CAs-ZIF-8@MM-MOF}) - E(\text{CAs-ZIF-8@MM-MOF}) - E(\text{Fe}) - n\mu(\text{H})$$

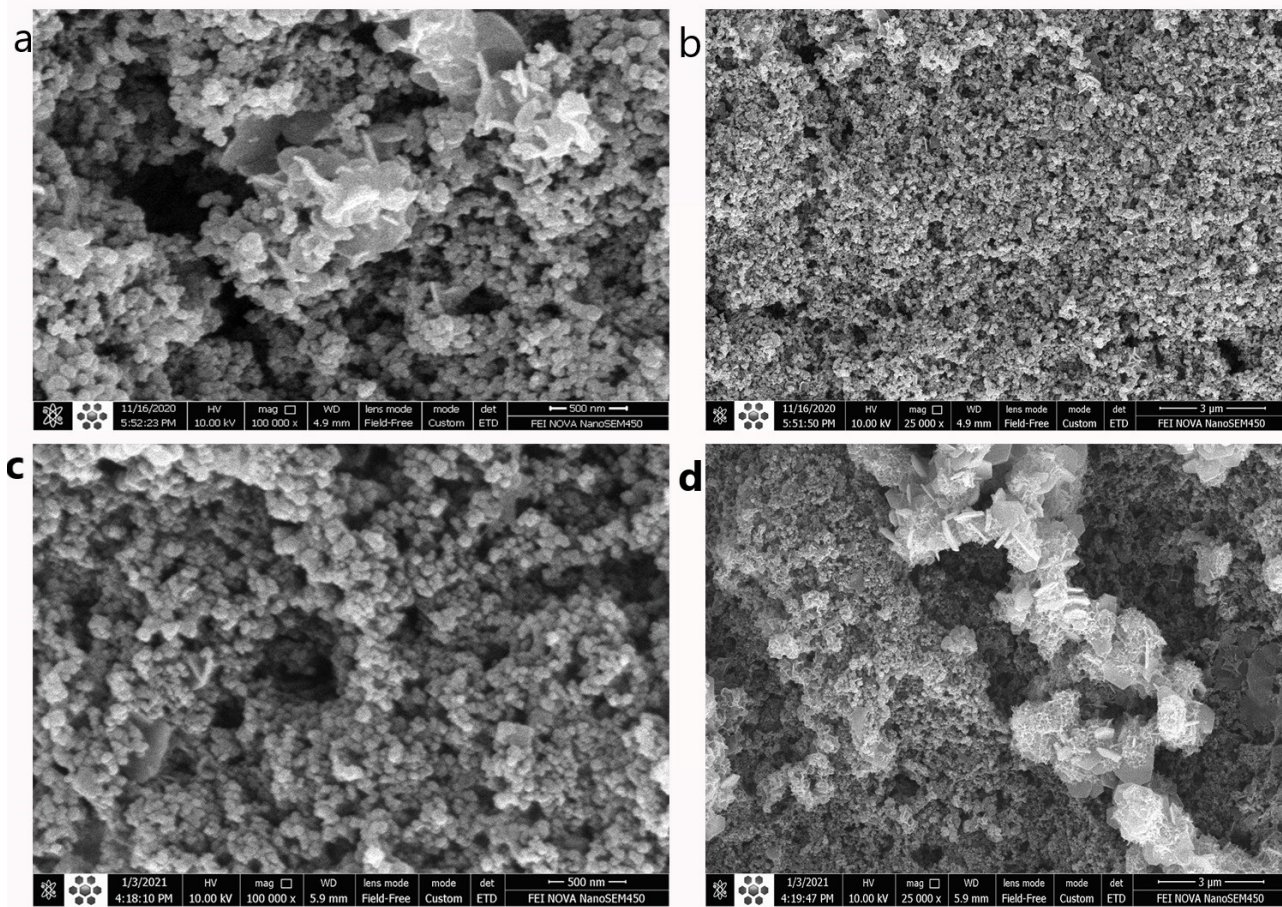
E is the total energy of related systems and  $\mu$  (H) is the total energy per H atom and defined as  $\mu$  (H<sub>2</sub>)/2, n is the number of substituted H.

Moreover, the adsorption energy of H<sub>2</sub>S was calculated as follows:

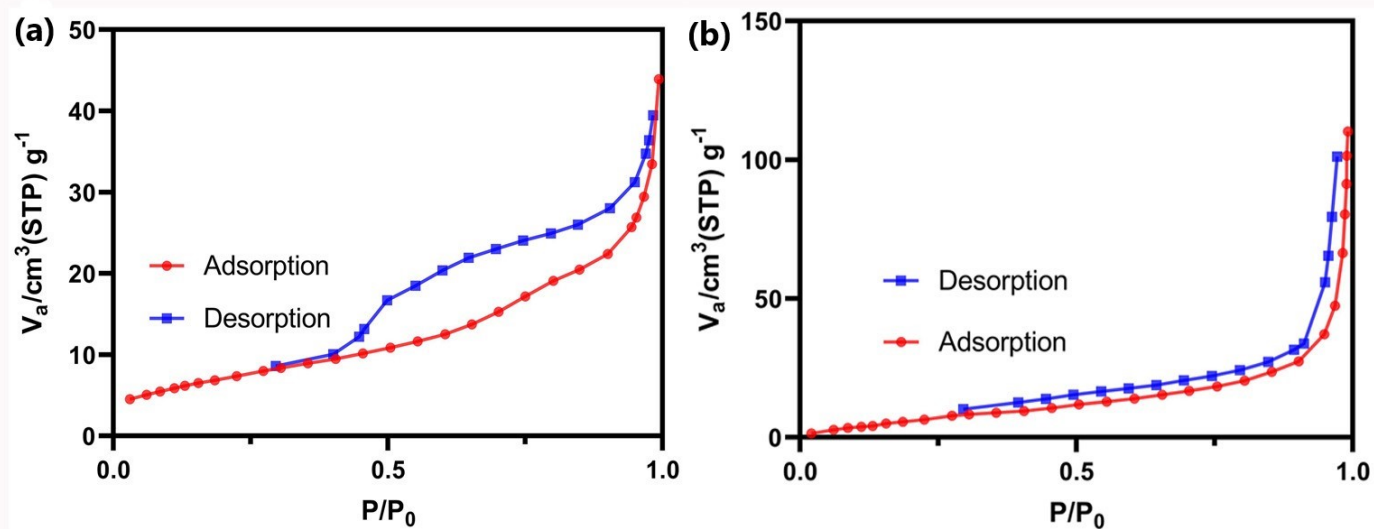
$$E_{\text{ads}} = E_{\text{slab+ mol}} - E_{\text{slab}} - E_{\text{mol}}$$

Where  $E_{\text{slab+ mol}}$  is the total energy of slab after adsorption,  $E_{\text{slab}}$  is the energy of Fe-doped CAs-ZIF-8@MM-MOF or CAs-ZIF-8@MM-MOF, and the  $E_{\text{mol}}$  is the total energy of H<sub>2</sub>S.

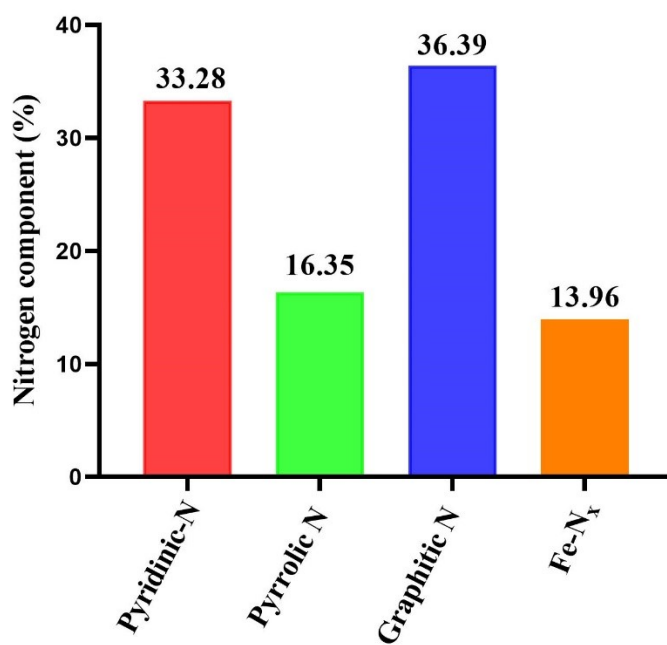
## 2. Supplementary Figures



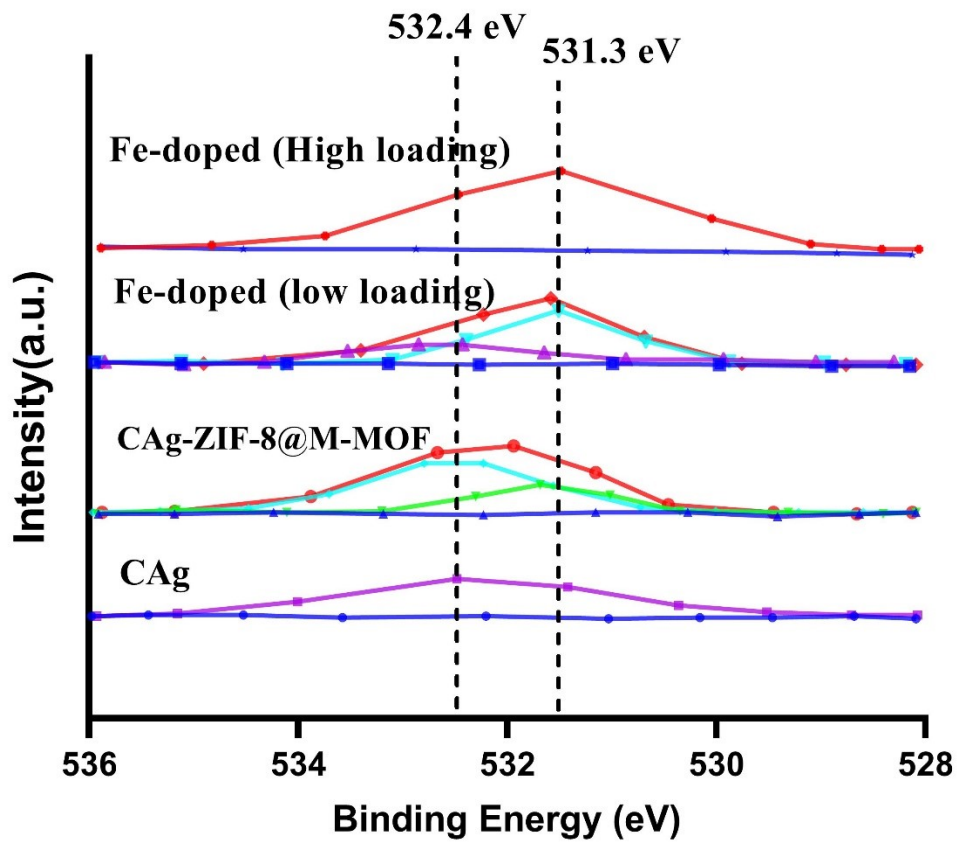
**Supplementary Figure S1:** FE-SEM images of Fe-doped CAs-ZIF-8@MM-MOF before (a, b) and after H<sub>2</sub>S oxidation (c, d).



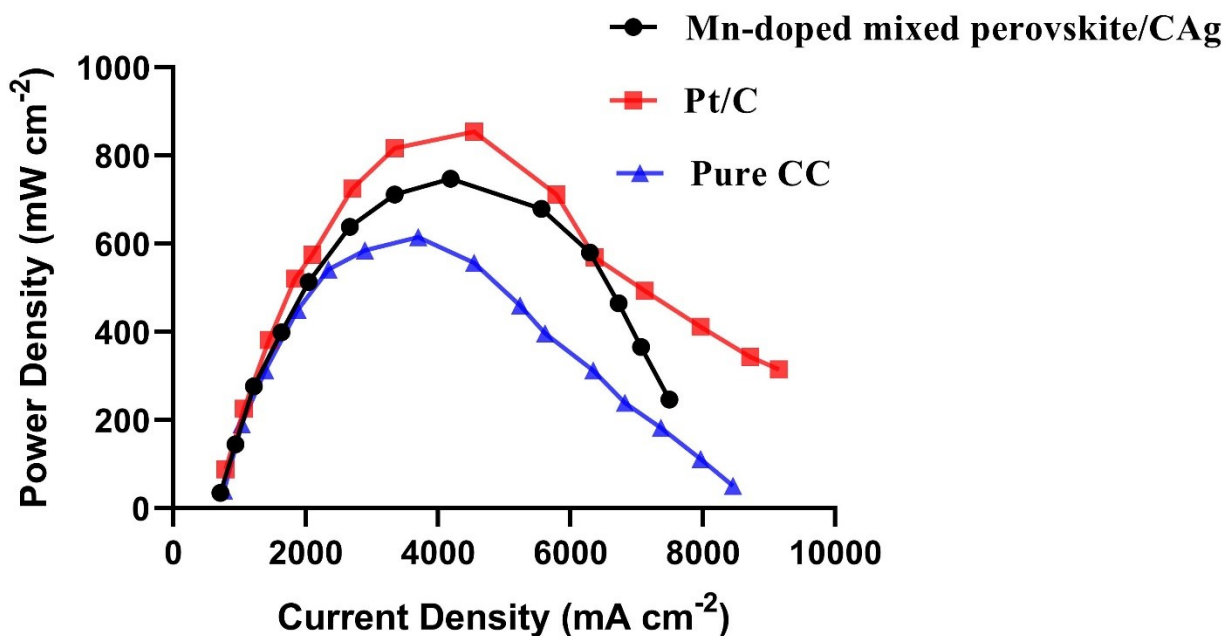
**Supplementary Figure S2:** N<sub>2</sub> Adsorption and desorption isotherms of Fe-doped CAs-ZIF-8@MM-MOF before (a) and after (b) H<sub>2</sub>S electro-oxidation.



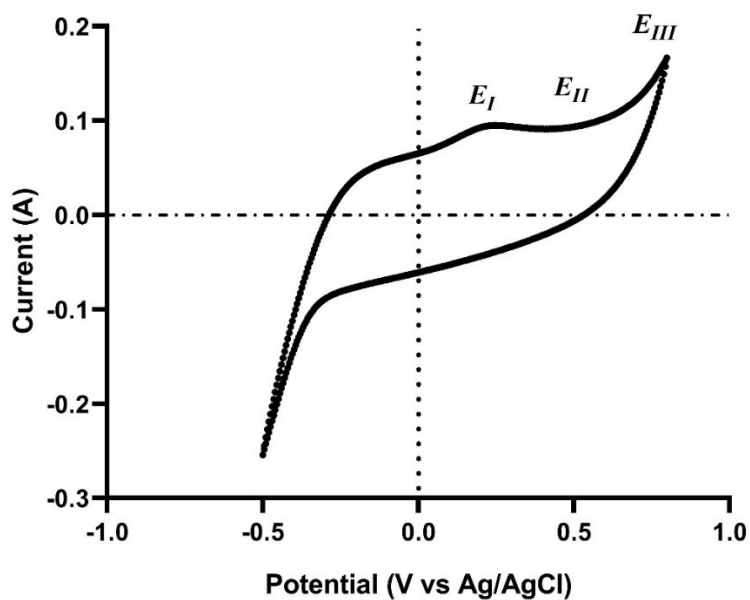
**Supplementary Figure S3:** the content of different nitrogen species for Fe-doped CAs-ZIF-8@MM-MOF electro-catalyst.



*Supplementary Figure S4:* XPS O1s spectra of the as-prepared catalysts.

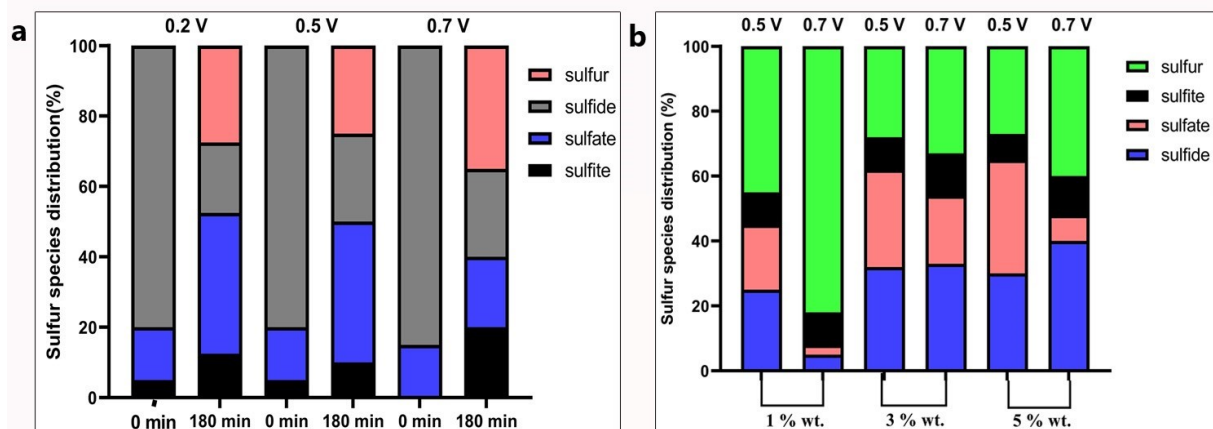


*Supplementary Figure S5:* Obtained power density curves in 50 mM phosphate buffer solution (PBS) for as-synthesized catalysts.

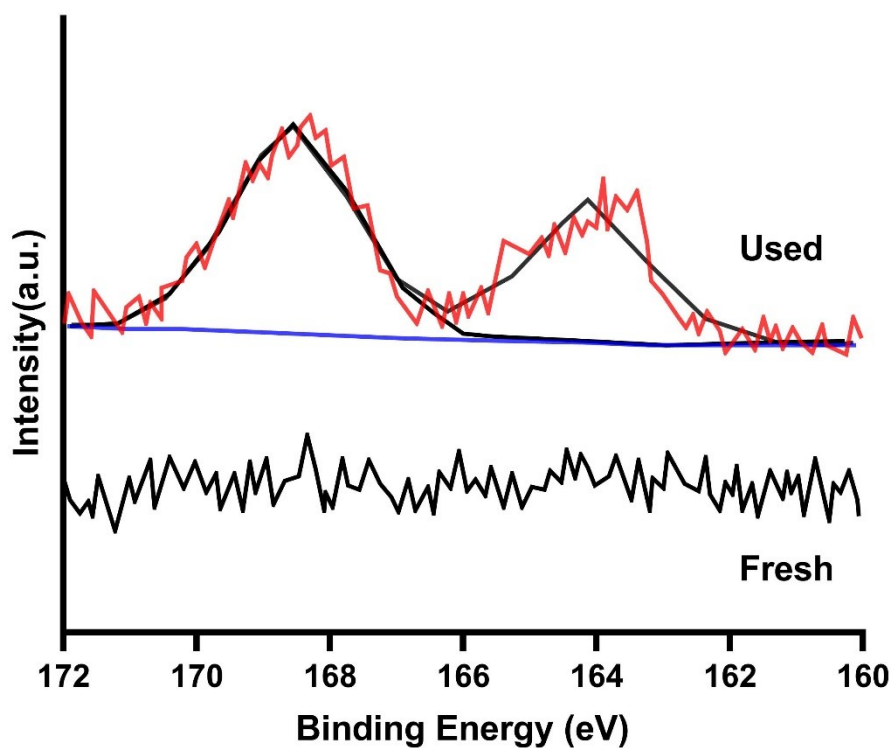


*Supplementary Figure S6:* Cyclic voltammetry (CV) tests carried out at Fe-doped CAs-ZIF-8@MM-MOF/CC electrode in the 2.8 mM H<sub>2</sub>S (HS<sup>-</sup>) solution at pH 8.



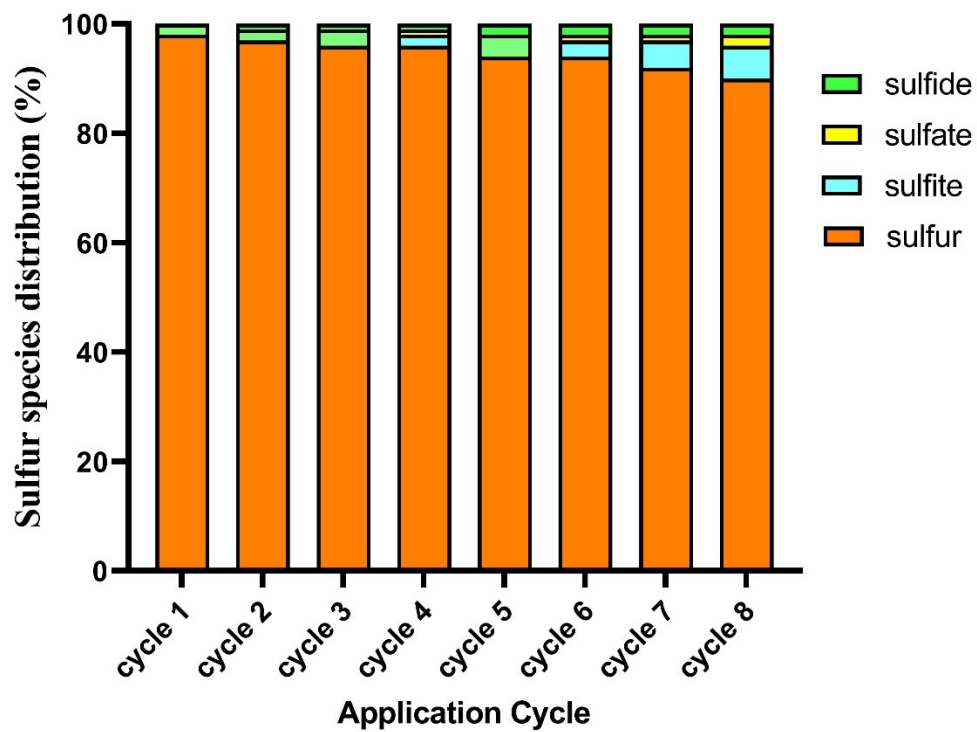


**Supplementary Figure S7:** First-order  $\text{H}_2\text{S}$  removal rates ( $\text{h}^{-1}$ ) at different anode potentials at (a) carbon cloth (CC) electrode; and (b) Fe-doped CAS-ZIF8@MM-MOF/CC electrode.

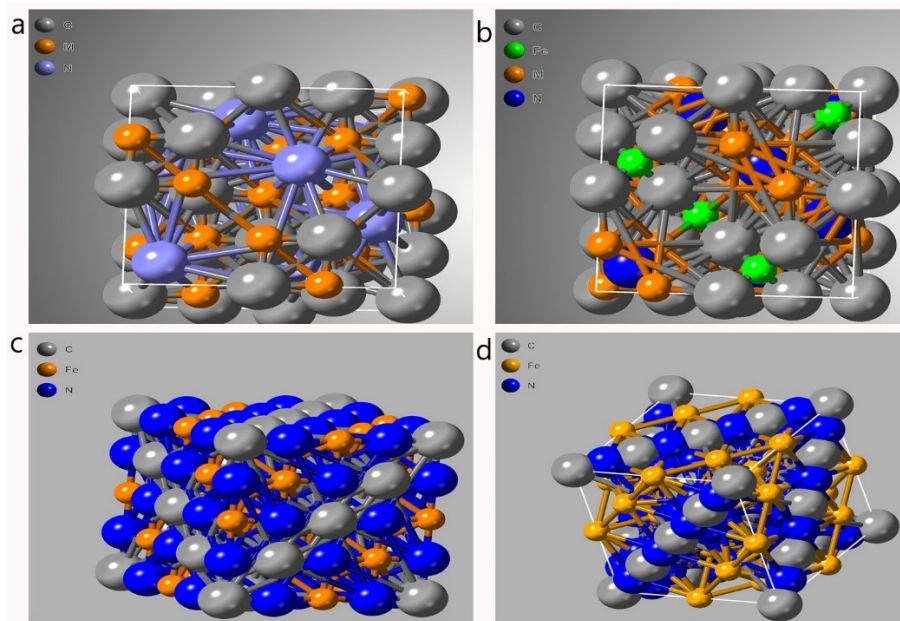


**Supplementary Figure S8:** XPS S 2p spectra of used and fresh Fe-doped CAS-ZIF-8@MM-MOF.

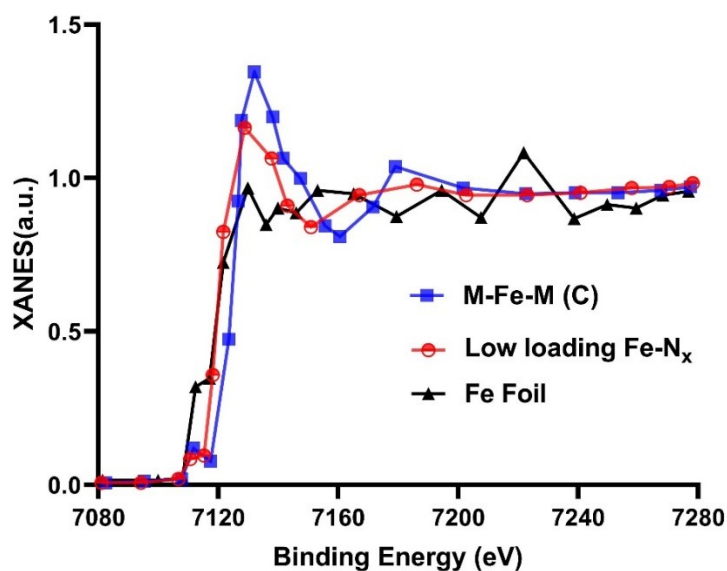




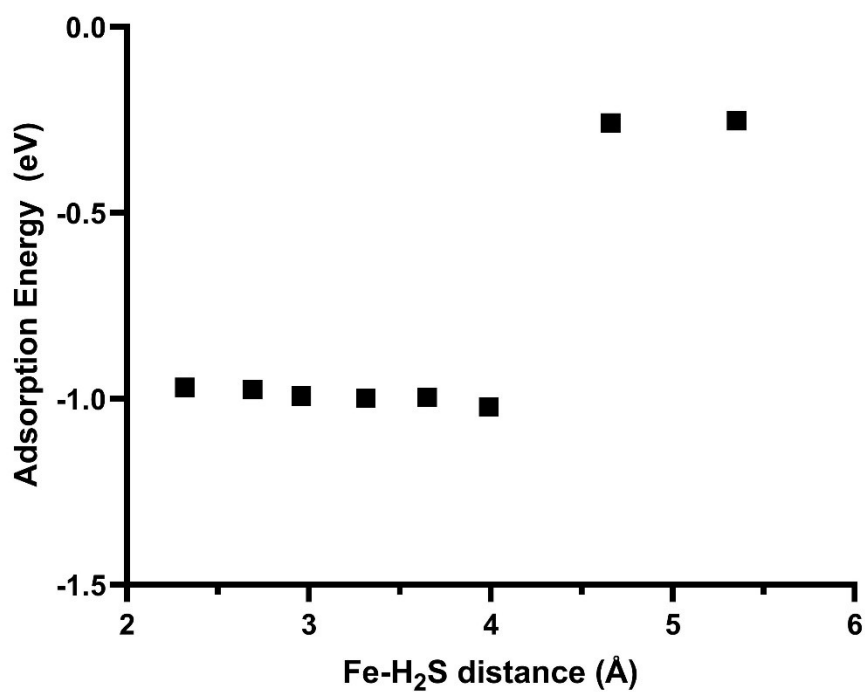
*Supplementary Figure S9:* the distribution of sulfur species in repeated cycles for H<sub>2</sub>S removal and stability of used Fe-doped CAs-ZIF-8@MM-MOF.



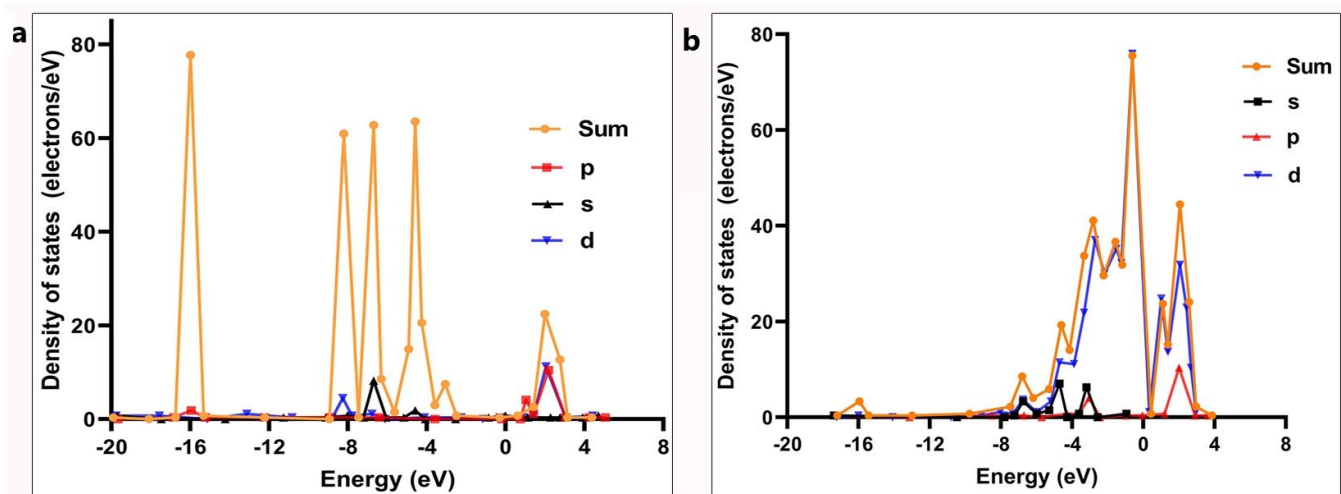
**Supplementary Figure S10:** the general and optimized configuration of Fe-doped CAS-ZIF-8@MM-MOF of before doping (a) and after doping (b) and also under low loading of Fe nanoparticles (c) and high loading of Fe nanoparticles (d).



**Supplementary Figure S11:** Fe K-edge XANES of proposed configuration for Fe-doped CAS-ZIF-8@MM-MOF.



**Supplementary Figure S12:**  $E_{\text{ads}}$  of H<sub>2</sub>S on the Fe-doped CAs-ZIF-8@MM-MOF (Fe-N<sub>4</sub>) in different H<sub>2</sub>S-Fe distances.



**Supplementary Figure S13:** the electron transfer of the S of H<sub>2</sub>S and Fe in the Fe-N<sub>4</sub> configuration for the Fe-doped CAs-ZIF-8@MM-MOF/H<sub>2</sub>S system obtained from the DOS (a) and PDOS (b).

### 3. Supplementary Tables

**Supplementary Table S1:** EDX elemental analysis of Fe-doped CAs-ZIF-8@MM-MOF catalyst.

Type operation	The elements	% wt.	% At.
Before oxidation	C	88.95	93.25
	Fe	6.78	4.1
	Co	2.58	1.17
	Mn	0.46	0.31
	Sr	1.23	1.17
After oxidation	C	87.26	95.32
	Fe	6.74	2.11
	Co	2.41	0.98
	Mn	0.41	0.11
	Sr	1.19	0.46
	S	1.99	1.02

**Supplementary Table S2:** Total dissolved Iron concentration of Fe-doped CAs-ZIF-8@MM-MOF for stability testing at 0.5 V and 0.7 V vs SHE.

Time (h)	Total dissolved Fe (mg L <sup>-1</sup> )	
	0.5 V	0.7 V
0	0.02	0.04
2	0.08	0.13
4	0.07	0.11

**Supplementary Table S3:** First-order constant removal rates ( $\text{h}^{-1}$ ) at CC and Fe-doped CAs-ZIF-8@MM-MOF/CC electrodes obtained at the different anodic potentials.

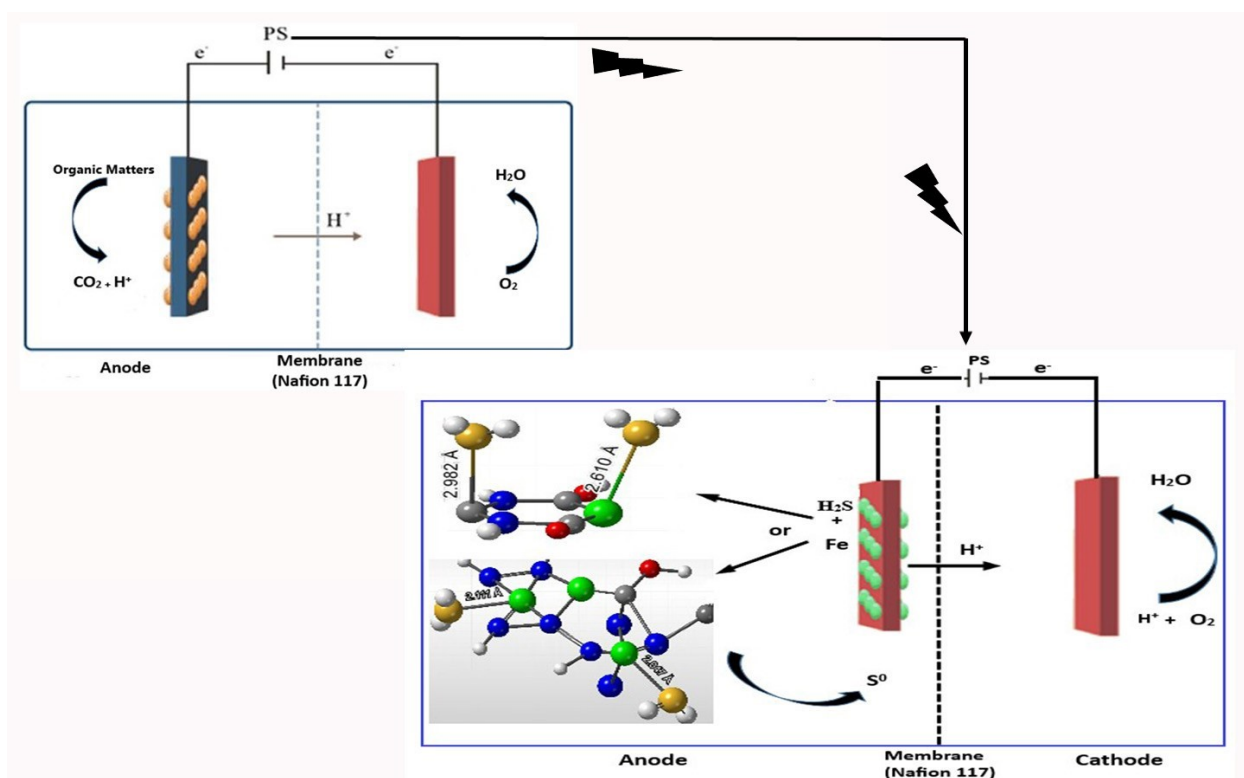
Type of used electrode	Time (h)	Applied Potential (V)	Loading of Fe nanoparticles (% wt.)	First-order removal rate ( $\text{h}^{-1}$ )
Pure CC	2 h	0.2	-	0.54
		0.5	-	0.79
		0.7	-	1.13
Fe-doped CAs-ZIF-8@MM-MOF	2 h	0.5	1	4.18
			3	2.58
			5	2.38
		0.7	1	8.12
			3	2.34
			5	4.48

**Supplementary Table S4:** The bond distance in the catalysts before and after Fe nanoparticles doping

The catalysts	Type of coordination environment	Type of Bonding	Bond length
CAs-ZIF-8@MM-MOF	M-C-N	M-C	1.42625
		M-C	1.46340
		M-C	1.48454
		M-C	2.51235
		M-C	2.53214
Fe-doping CAs-ZIF-8@MM-MOF	M-Fe-M(C)	M-C	1.31132
		M-C	1.34232
		M-C	1.36252
		M-C	2.38632
		M-C	2.41254
		Fe-C	1.23517
		Fe-C	1.25325
		M-Fe	1.23522
		M-Fe	2.36517
Fe-doping CAs-ZIF-8@MM-MOF (low)	Fe-N <sub>4</sub>	Fe-N	1.42625
		Fe-N	1.45256
		Fe-N	1.47034
		Fe -C	2.01702

Fe-doping CAs-ZIF-8@MM-MOF (high loading of Fe)	Fe-N <sub>4</sub> -C	Fe -C	2.41500
		Fe -C	2.85250
	Fe-N <sub>4</sub>	Fe-N	1.74679
		Fe-Fe	2.25510
	Fe-N <sub>4</sub> -C	Fe-Fe	2.66827
		Fe -C	2.01702
Fe -C		2.85250	
		Fe -C	3.49358

#### 4. Supplementary scheme 1



### ***Supplementary References***

1. Jia, Mei-ye, Sheng-gui He, and Mao-fa Ge. "Experimental and Theoretical Study of Reactions between Manganese Oxide Cluster Cations and Hydrogen Sulfide." *Chinese Journal of Chemical Physics* 26.6 (2014): 679.
2. Yan, Yimin, et al. "Bimetallic organic framework-derived, oxygen-defect-rich  $\text{Fe}_x\text{Co}_{3-x}\text{S}_4/\text{Fe}_y\text{Co}_{9-y}\text{S}_8$  heterostructure microsphere as a highly efficient and robust cathodic catalyst in the microbial fuel cell." *Journal of Power Sources* 472 (2020): 228582.
3. Yun, Yapei, et al. "Design and remarkable efficiency of the robust sandwich cluster composite nanocatalysts ZIF-8@ Au<sub>25</sub>@ ZIF-67." *Journal of the American Chemical Society* 142.9 (2020): 4126-4130.
4. Lü, Baozhong, et al. "Fischer–Tropsch Synthesis: ZIF-8@ ZIF-67-Derived Cobalt Nanoparticle-Embedded NanoCAGE Catalysts." *Industrial & Engineering Chemistry Research* 59.27 (2020): 12352-12359.
5. Tran, Y. B. N., et al. "Series of MM-MOF-184 (M= Mg, Co, Ni, Zn, Cu, Fe) Metal–Organic Frameworks for Catalysis Cycloaddition of CO<sub>2</sub>." *Inorganic Chemistry* 59.22 (2020): 16747-16759.
6. Zhang, Minhua, et al. "The modified MOF-74 with H<sub>2</sub> dissociation function for CO<sub>2</sub> hydrogenation: A DFT study." *Materials Today Communications* 27 (2021): 102419.